

1 **Supplemental Material**

2

3 **MATERIALS AND METHODS**

4

5 ***Microbubble Formulations***

6 Microbubbles were composed of decafluorobutane gas core and the following base lipid  
7 components: phosphatidylcholine (2mg/ml) and polyethylene glycol stearate (2mg/ml). Rapamycin (0.4  
8 mg/ml) was added to the base components to produce therapeutic microbubbles. A trace amount of the  
9 fluorescent dye DiI (Molecular Probes, Eugene, OR) was added to the base components to produce  
10 control microbubbles with fluorescent shell. To remove excess rapamycin, DiI, or lipids from the aqueous  
11 media, all microbubbles were washed by centrifugal flotation prior to injection into the animals.  
12 Measurement of the microbubble concentration was performed by a Coulter Counter (Multisizer III,  
13 Beckman Coulter, Brea, CA) before injection. The final concentration of rapamycin in the microbubbles  
14 prior to injection was previously determined to be 29ng per million microbubbles <sup>1</sup>.

15

16 ***Balloon Angioplasty in the Rat Carotid Artery***

17 Carotid balloon injury is a common arterial stenosis model and yields a highly reproducible  
18 neointima at various time points <sup>2</sup>. All animal experiments were conducted under University of Virginia  
19 Animal Care and Use Committee (ACUC) approved protocols. Rats were anesthetized with isoflurane in  
20 a gas induction chamber, and kept under anesthesia for the duration of the surgical procedure. The hair  
21 on the neck was removed and the area sterilized with betadine and ethanol. An incision was made down  
22 the center of the neck. Guide sutures were placed around the left jugular vein. Next, the right carotid was  
23 located and temporary ligatures were placed around the internal and external branches of the right carotid,  
24 and along the proximal end of the right carotid. Before insertion, a 2F Fogarty balloon catheter (Edwards  
25 Lifesciences, Irvine, CA), was filled with saline and pre-stretched to a volume of 0.04ml. The diameter of  
26 the balloon at this volume was approximately 4mm. A small incision was made in the right external

1 carotid, and the balloon catheter was immediately inserted. The balloon was then advanced to the right  
2 common carotid to a depth of 1.5cm at which point the balloon was inflated again to 0.04ml, and then  
3 pulled back to the bifurcation and deflated. The inflation process was repeated twice more for a total of 3  
4 passes through the artery. This process induces injury that leads to formation of a neointima. The balloon  
5 catheter was then removed and the right external carotid was permanently tied off. A polyethylene tubing  
6 catheter was inserted into the left jugular to serve as a microbubble injection port. The incision was then  
7 temporarily closed so that sterility could be maintained during coupling with ultrasound gel and the  
8 transducers. At the conclusion of the study, the jugular catheter was removed, and the incision was  
9 stitched back together. For chronic studies, animals were allowed to recover in a heated chamber and  
10 were given Buprenex after initial recovery and 24 hours later.

11

### 12 ***Selection of Ultrasound Parameters for Rupture and Radiation Force***

13 Microbubbles in the 1-5  $\mu\text{m}$  range, like those used herein, are well suited for radiation force  
14 pushing and imaging <sup>3</sup>. Radiation force, or primary Bjerknes force, refers to the directional forces  
15 experienced by fluid or other media in an ultrasound field. It does not involve ionizing radiation. A  
16 model of radiation force ultrasound <sup>4</sup> was used to select acoustic parameters necessary for pushing  
17 microbubbles out of arterial blood flow without MB rupture. In order to achieve translation of  
18 microbubbles, continuous, 1.2 MHz sinusoidal radiation force pulses of ultrasound were applied at 135  
19 kPa (peak negative pressure). A 19mm unfocused 1MHz transducer was chosen in order to apply  
20 ultrasound over the entire length of the injured region of the artery.

21 The Sequoia 15L8 transducer (Siemens Medical Solutions, Malvern PA) and scanner were  
22 selected for their combined ability to image and emit destruction pulses. The contrast pulse sequence  
23 (CPS) mode <sup>5</sup> available on the Sequoia is specifically adapted for microbubble contrast imaging. Within  
24 this mode, the transducer can be programmed to emit 5MHz destruction pulses that rupture microbubbles.  
25 In this mode, the peak negative pressure of the pulse is approximately 1.5 MPa, and the five cycle pulse is  
26 repeated every 200 microseconds.

1

## 2 ***Ultrasound Mediated Delivery from Microbubbles In Vivo***

3           Freshly washed microbubbles were diluted to  $1 \times 10^9$  / mL of saline within 2 minutes of injection  
4 into the rat. For DiI microbubble delivery, a total of  $1 \times 10^9$  microbubbles were injected through the  
5 jugular vein. The same number of microbubbles had been injected I.V. into rats in previous studies <sup>6, 7</sup>,  
6 and corresponded to a total rapamycin dosage of 29  $\mu$ g per rat or 72.5  $\mu$ g/kg. For rapamycin microbubble  
7 delivery, either  $1 \times 10^8$  or  $1 \times 10^9$  microbubbles were injected to test the effect of microbubble dose on  
8 delivery efficacy with and without ultrasound.

9           Prior to microbubble injection, the ultrasound transducers were both coupled with gel, and  
10 aligned with the injured carotid artery. The 15L8 transducer was positioned vertically above the rat so  
11 that the injured portion of the artery and the bifurcation were in the field of view while in an imaging  
12 mode. The single element A314 (Olympus Panametrics-NDT, Waltham, MA) unfocused transducer was  
13 angled at a 45 degree angle from the 15L8 as shown in Fig. 1A. Both were positioned such that the  
14 injured artery was approximately 1 cm from the face of either transducer. The syringe containing 1 mL of  
15 microbubbles was gently rotated during the 5 minute injection period to prevent clumping inside the  
16 syringe. Upon initiation of microbubble infusion, the radiation force ultrasound was turned on and the  
17 15L8 was switched to burst mode and emitted pulses for 3 seconds, paused for 2 seconds, and repeated  
18 for the entire 8 minute exposure period. Unless otherwise noted, both radiation force and burst mode  
19 ultrasound were turned on simultaneously during the entire injection.

20

## 21 ***Tissue Harvesting and Processing***

22           For acute DiI delivery studies animals were immediately euthanized, and for chronic rapamycin  
23 delivery studies, animals were euthanized two weeks after the ultrasound mediated drug delivery (see Fig.  
24 1B). All animals were sacrificed by CO<sub>2</sub> inhalation and the chest was opened to induce bilateral  
25 pneumothorax. The vasculature was perfused with 15 mL of saline and then perfusion fixed with 15mL  
26 of 4% paraformaldehyde, and perfused once more with 15mL of saline. Both the right (injured) and left

1 (control) carotids were excised with the bifurcation, which served as a landmark. Arteries were  
2 immediately placed in fresh fixative overnight. The next day, arteries were transferred to 70% ethanol  
3 and processed for paraffin embedding. Paraffin embedding greatly reduces the DiI fluorescence in tissue,  
4 so carotids which underwent DiI microbubble delivery were instead placed in 30% sucrose solution  
5 overnight, followed by embedding in O.C.T. compound (Tissue-Tek, Torrance, CA), frozen on dry ice,  
6 and stored at -80°C before cryosectioning. All sections were cut in 5 μm thick slices and sections were  
7 made in 200 μm increments from the bifurcation.

8

### 9 *Histology and Quantification*

10 DiI delivery to carotid arteries was analyzed in 4-8 cryosections from each left (uninjured) and  
11 right (injured) carotid by fluorescence microscopy on a confocal microscope (FluoView, Olympus  
12 America Inc., Center Valley, PA). Elastic laminae were detected by autofluorescent green emission after  
13 exciting the tissue at 488 nm. DiI delivery was identified by excitation at 550nm. Images at 20x  
14 magnification were captured with an exposure time of 100ms for both red and green signals. A custom  
15 Matlab algorithm detected all fluorescent pixels above a background threshold in order to remove all  
16 background fluorescence. All measurements are listed in arbitrary fluorescence units.

17 Arteries from chronic rapamycin delivery studies were stained with hematoxylin and eosin in  
18 order to delineate the elastic lamina and neointima. The external elastic lamina (EEL), internal elastic  
19 lamina (IEL), and lumen borders were traced using ImageJ software (<http://rsbweb.nih.gov/ij/>). Slice  
20 sections between 2-5mm from the bifurcation were analyzed such that at least 16 slices were analyzed per  
21 artery. The area inside each perimeter trace was used to calculate the area of the media and the  
22 neointima. To adjust for differences in sizes of the rats, the ratio of neointima to media was calculated for  
23 each rat.

24 An apoptosis stain was performed on artery sections of four of the rats within each of the  
25 following rapamycin delivery groups: balloon injury only, balloon injury with  $10^9$  rapamycin  
26 microbubbles, and balloon injury with  $10^9$  rapamycin microbubbles and ultrasound. Terminal

1 deoxynucleotidyl transferase-mediated dUTP-biotin nick end labeling (TUNEL) was applied to detect  
2 apoptotic cells in at least 8 slice sections per artery. TUNEL staining was performed using an ApopTag  
3 kit (Chemicon International, Billerica, MA). All histomorphometric parameters were analyzed by  
4 experienced investigators.

5

### 6 ***Statistical Analysis***

7 Statistical significance for all studies was determined with two-sided t-tests assuming equal variance.  
8 A p value less than 0.05 was considered to indicate a statistically significant difference. To determine  
9 therapeutic efficacy in the animal study, an ANOVA test was first performed to determine the  
10 significance between insonated and non-insonated groups and resulted in a p-value of less than  $1 \times 10^{-5}$  ( $P$   
11 =  $8.943 \times 10^{-5}$ ). The data in the groups also passed a normal distribution test. From this, a post-hoc  
12 analysis using a non-paired, two-sided t-test was performed so that individual differences between each  
13 set of animals could be further analyzed.

14

15

## 16 **RESULTS**

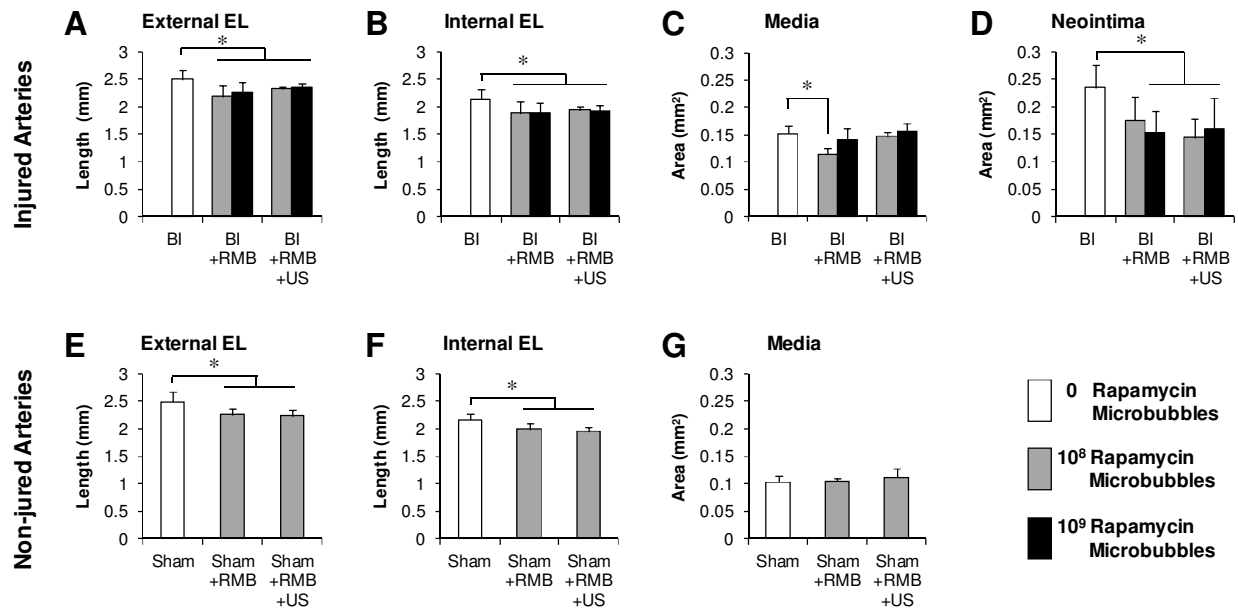
17 The neointima to media ratios for each artery were calculated from the perimeter traces of the  
18 external elastic lamina (EEL) and internal elastic lamina (IEL). The lengths of the EEL and IEL were  
19 also measured (Supp. Fig. 1A,B). Of the injured arteries, only the balloon injury group had significantly  
20 longer EEL and IEL lengths than any other treated group. This difference was also observed between  
21 contralateral non-injured sham arteries (Supp. Fig. 1E,F). Although none of the sham arteries were  
22 injured, those that were never exposed to any RMBs were slightly larger suggesting that this group of  
23 animals was slightly larger. The area of the media in each treatment group was similar with the exception  
24 of the arteries treated with  $10^8$  RMBs without ultrasound (Supp. Fig. 1C). A similar pattern was observed  
25 among the medial areas of the contralateral non-injured (sham) arteries, but was not statistically  
26 correlative (Supp. Fig. 1G). The medial areas of the sham arteries were all smaller than those of the

1 injured arteries, as is expected in a balloon injury model. In order to reduce any differential effects from  
 2 variations in sizes of the rats, the neointimal area (Supp. Fig. 1D) of each rat was compared to its  
 3 corresponding medial area. In doing so, the neointima to media (NI/M) ratios for each treatment group  
 4 were calculated; these are listed in Supplemental Table I. No neointima formation was observed in non-  
 5 injured (sham) arteries.

6  
 7 **Supplemental Table I:** Neointima to Media ratios of Balloon Injured Arteries Treated with or without  
 8 rapamycin microbubbles or ultrasound

	NI/M (mean ± S.D.)	p	n
<b>BI</b>	1.54 ± 0.25	n/a	11
<b>BI + 1e8 RMB</b>	1.54 ± 0.32	0.9952	6
<b>BI + 1e9 RMB</b>	1.10 ± 0.16	0.0009	7
<b>BI + 1e8 RMB + US</b>	0.99 ± 0.24	0.0006	6
<b>BI + 1e9 RMB + US</b>	1.01 ± 0.33	0.0013	7

9



10

11 **Supplemental Figure I:** Comparison of carotids at two weeks post balloon injury (BI) following  
 12 treatment with low (10<sup>8</sup>) or high (10<sup>9</sup>) dose of rapamycin microbubbles (RMB), with or without  
 13 ultrasound. The perimeters and areas of the **A**) external elastic lamina (EEL), **B**) internal elastic lamina

1 (IEL) and the lumen were measured to calculate the areas of the C) media and D) neointima. E,F,G)  
2 Contralateral control arteries in the same animals represent shams, and no ultrasound was applied directly  
3 to them, but are demarcated by "+US" to indicate that ultrasound was applied to the injured right carotid  
4 arteries in the same animals. Neointima to media (NI/M) ratio was reduced with and without ultrasound  
5 for the high RMB dose, but was significantly reduced (35%) by the low dose of RMB only when  
6 ultrasound was applied ( $n \geq 6$ , data presented as mean  $\pm$  S.D., \* $p < 0.05$  compared to BI alone).

7

8

## 9 DISCUSSION

10 Several other studies have shown similar levels of decreased hyperplasia after higher doses of  
11 rapamycin delivery. In a seminal study by Gregory *et al*<sup>8</sup> rapamycin was injected intraperitoneally into  
12 rats which had undergone carotid balloon injury. A dose of 1.5mg/kg was injected each day for 14 days.  
13 After 14 days neointimal thickening was reduced by 45%. It is important to note that side effects are  
14 associated with injection of more than 2mg of rapamycin in humans<sup>9</sup>. In the studies presented herein,  
15 neointimal thickening was reduced by at least 35% after a single treatment of ultrasound with rapamycin  
16 microbubbles containing only 0.73 $\mu$ g/kg - over 2000 times less. Parry *et al* applied 200 $\mu$ g of rapamycin  
17 perivascularly to balloon injured carotids in 350 kg rats. This was almost 7 times more rapamycin than  
18 was injected in the present study. At 14 days post injury neointimal cross sectional area was reduced by  
19 approximately 75%. One study, in which an I.V. rapamycin dose of ~8  $\mu$ g/kg was injected in a porcine  
20 stent model, resulted in reduction of neointima formation without ultrasound application<sup>10</sup>. Similarly, the  
21 neointima formation within arteries of the present study was reduced after injection of the high dose of  
22 RMBs (containing 7.3 $\mu$ g rapamycin/kg) even without ultrasound. Large doses of rapamycin are  
23 sufficient to reduce injury induced stenosis, however, our ultrasound mediated delivery from  
24 microbubbles allows for at least 10 fold lower doses to be injected with equivalent therapeutic responses.

25 TUNEL staining revealed low levels of apoptotic cells in all three injured artery treatment groups.  
26 These low levels are consistent with basal levels of cell turnover<sup>11</sup> and account for less than 0.01% of the

1 cells in the intima and less than 0.1% of the cells in the media. It is possible that more apoptosis occurred  
2 within the first few days after injury. As reported by Ferns and Avades <sup>12</sup>, the majority of apoptosis  
3 occurs within the first several days following balloon injury.

4 This method can also be employed in other arterial beds such as the coronary arteries <sup>13</sup>. Using  
5 intravascular ultrasound from a modified catheter we previously performed gene delivery *in vivo* in  
6 porcine coronary arteries. Studies by Patil et al have demonstrated the ability of ultrasound to push  
7 microbubbles and deliver reagents to large blood vessel walls<sup>14</sup>.

8  
9

## 10 REFERENCES

- 11 1. Phillips LC, Klivanov AL, Wamhoff BR, Hossack JA. Localized ultrasound enhances delivery of  
12 rapamycin from microbubbles to prevent smooth muscle proliferation. *J. Control. Release.* 2011
- 13 2. Clowes AW, Reidy MA, Clowes MM. Mechanisms of stenosis after arterial injury. *Laboratory*  
14 *Investigation.* 1983;49:208-215
- 15 3. Patil AV, Rychak JJ, Allen JS, Klivanov AL, Hossack JA. Dual frequency method for  
16 simultaneous translation and real-time imaging of ultrasound contrast agents within large blood  
17 vessels. *Ultrasound in Medicine and Biology.* 2009;35:2021-2030
- 18 4. Dayton PA, Allen JS, Ferrara KW. The magnitude of radiation force on ultrasound contrast  
19 agents. *Journal of the Acoustical Society of America.* 2002;112:2183-2192
- 20 5. Phillips PJ. Contrast pulse sequences (cps): Imaging nonlinear microbubbles. *Ultrasonics*  
21 *Symposium, 2001 IEEE.* 2001;2:1739-1745 vol.1732
- 22 6. Christiansen JP, French BA, Klivanov AL, Kaul S, Lindner JR. Targeted tissue transfection with  
23 ultrasound destruction of plasmid-bearing cationic microbubbles. *Ultrasound in Medicine and*  
24 *Biology.* 2003;29:1759-1767
- 25 7. Zhou J, Wang YX, Xiong YF, Wang HX, Feng YM, Chen JA. Delivery of tfpi-2 using ultrasound  
26 with a microbubble agent (sonovue) inhibits intimal hyperplasia after balloon injury in a rabbit  
27 carotid artery model. *Ultrasound in Medicine and Biology.* 2010;36:1876-1883
- 28 8. Gregory CR, Huie P, Billingham ME, Morris RE. Rapamycin inhibits arterial intimal thickening  
29 caused by both alloimmune and mechanical injury - its effect on cellular, growth-factor, and  
30 cytokine responses in injured vessels. *Transplantation.* 1993;55:1409-1418
- 31 9. Mahalati K, Kahan BD. Clinical pharmacokinetics of sirolimus. *Clinical Pharmacokinetics.*  
32 2001;40:573-585
- 33 10. Kipshidze NN, Porter TR, Dangas G, Yazdi H, Tio F, Xie F, Hellinga D, Wolfram R, Seabron R,  
34 Waksman R, Abizaid A, Roubin G, Iyer S, Colombo A, Leon MB, Moses JW, Iversen P. Novel  
35 site-specific systemic delivery of rapamycin with perfluorobutane gas microbubble carrier  
36 reduced neointimal formation in a porcine coronary restenosis model. *Catheterization and*  
37 *Cardiovascular Interventions.* 2005;64:389-394
- 38 11. Han DKM, Haudenschild CC, Hong MK, Tinkle BT, Leon MB, Liau G. Evidence for apoptosis  
39 in human atherogenesis and in a rat vascular injury model. *American Journal of Pathology.*  
40 1995;147:267-277



1 12. Ferns GAA, Avades TY. The mechanisms of coronary restenosis: Insights from experimental  
2 models. *International Journal of Experimental Pathology*. 2000;81:63-88  
3 13. Phillips LC, Klibanov AL, Bowles DK, Ragosta M, Hossack JA, Wamhoff BR. Focused in vivo  
4 delivery of plasmid dna to the porcine vascular wall via intravascular ultrasound destruction of  
5 microbubbles. *Journal of Vascular Research*. 2010;47:270-274  
6 14. Patil AV, Rychak JJ, Klibanov AL, Hossack JA. Real-time technique for improving molecular  
7 imaging and guiding drug delivery in large blood vessels: In vitro and ex vivo results. *Mol*  
8 *Imaging*. 2011;10:238-247  
9  
10